Cost-efficient deep learning method for mass inverse design of photonic devices

Arthur Clini de Souza, Paloma Elias da Silva Pellegrini, Silvia Vaz Guerra Nista, Stéphane Lanteri, Hugo Enrique Hernandez-Figueroa, Marco Abbarchi, Badre Kerzabi, Mahmoud Elsawy

Cost-Efficient Deep Learning Method for Mass Inverse Design of Photonic Devices

Arthur Clini de Souza
Université Côte d'Azur, Inria, CNRS, LJAD, 06902 Sophia Antipolis Cedex, France
Solnil, 95 Rue de la République, 13002 Marseille, France

Paloma Elias da Silva Pellegrini
University of Campinas (UNICAMP)
Campinas, São Paulo, Brazil

Silvia Vaz Guerra Nista
University of Campinas (UNICAMP)
Campinas, São Paulo, Brazil

Stéphane Lanteri
Université Côte d'Azur, Inria, CNRS, LJAD,
06902 Sophia Antipolis Cedex, France

Hugo Enrique Hernandez-Figueroa
University of Campinas (UNICAMP)
Campinas, São Paulo, Brazil

Marco Abbarchi
Solnil, 95 Rue de la République, 13002 Marseille, France
Université Aix Marseille, CNRS, Université de Toulon, IM2NP, UMR 7334
F-13397 Marseille, France

Badre Kerzabi
Solnil, 95 Rue de la République
13002 Marseille, France

Mahmoud Elsawy*
Université Côte d'Azur, Inria, CNRS, LJAD,
06902 Sophia Antipolis Cedex, France
*mahmoud.elsawy@inria.fr

***Abstract*—We apply an efficient inverse design methodology to conceive metasurface-based beam deflectors. We start by creating a small dataset composed by the results of simple simulations to train two deep neural networks. Once the models are trained, various beam deflectors can be inverse designed without further full-wave simulations. Our approach combines physical intuition about blazed gratings with a state-of-the-art optimization methodology, achieving high efficiencies while requiring modest computational effort. One design was successfully fabricated using sub-20 nm thermal scanning probe lithography.**

***Index Terms*—Deep Learning, Optimization, Inverse Design, Metasurfaces, Lithography.**

I. Introduction

Metasurfaces are the two-dimensional analogous of metamaterials, having sub-wavelength elements that control the light waves [1]. They can be used for a wide range of applications, such as structural color filtering [2], [3], meta-lenses for planar optics [4], [5] and holography [6]. Depending on the specific application and the type of metasurface, the inverse design process may necessitate the use of optimization algorithms. Currently, the literature offers a diverse range of algorithms, some tailored to optimize particular types of devices, while others offering more general uses [7]. With the rise of machine learning with deep neural networks (DL), many studies focus on DL's capabilities for efficient inverse design [8].

Here we leverage a DL optimization algorithm [2], [9] to design metasurface-based beam deflectors [10] operating in reflection mode, where incident light at 630 nm with an 80-degree angle of incidence is reflected to a desired angle. The advantage of the proposed algorithm lies in its versatility. Once simulations are completed and the models trained, no further simulations are necessary. Inverse design is then reduced to simply providing the desired target response. Out of the 200 different designs conceived by the algorithm, one was fabricated using a high resolution lithography, as proof of concept [11].

Funding obtained by CNPq processes 407839/2023-2 and 406193/2022-3.

II. Optimization Methodology

The methodology follows a similar line of previous works [2], [9]. It starts by generating a dataset to train a neural network surrogate model. The schematic of the simulations is shown in Fig. 1. Due to fabrication limitations, the height H was fixed to 150 nm, the metal was aluminium and the meta-atoms were made of titania (TiO_2). The device was covered by a layer of polymethyl (methacrylate-co-methacrylic acid) (PMMA/MA) for protection. The optimized variables were the pitch (P), the filling fraction (FF) and the thickness of the PMMA/MA layer above the resonator (T). The diffracted angles targets vary from -35° to 35° and according to the grating equation $P = -m\lambda/(\sin\theta_i - \sin\theta_m)$, where λ is the wavelength, m is the diffraction order, $\theta_i = 80^\circ$ is the incident angle and θ_m is the angle of the m^{th} diffraction order mode, considering $\theta_{m=-1}$ implies spanning P from $400\,\text{nm}$ to $1600\,\text{nm}$; the FF spans from 10% to 90% which would require a lithography resolution of up to $40\,\text{nm}$, not far form our experimental limit; T spans from $40\,\text{nm}$ to $200\,\text{nm}$.

We generated 1000 different geometries sampled from Halton sequence with Owen scrambling [12], [13] in order to have an even filling of the design space. The incident light is s-polarized with 80 degrees of incident angle and 630 nm of wavelength. The total simulation time was 37 minutes and 46 seconds.

We employed a data augmentation technique where we utilize the scattering angle as an input to the surrogate model. However, diffraction angles on periodic structures are discrete, and therefore, to create a more tangible dataset for a neural network to learn, we added an artificial Full Width at Half Maximum (FWHM) at each diffraction angle. Fig. 2 shows a schematic of the deep neural network surrogate model used.

The next step is training a Multi-Valued Artificial Neural Network (MVANN). Which is a neural neural network with multiple inputs [9]. Where the inputs are the target responses and the output are the parameters. In this study we used surrogate losses and 25 outputs,

979-8-3503-8817-6/24/$31.00 ©2024 IEEE

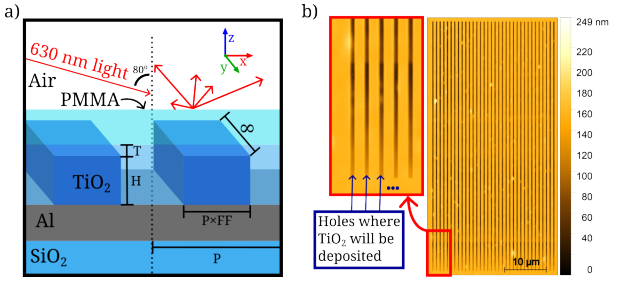

Fig. 1. a) Schematic of the simulated device. Slabs of TiO_2 (refractive index: 2.5 @ 630 nm) are positioned above a sheet of 300 nm of Al over a substrate of SiO_2. The resonators are protected with a layer of PMMA/MA (refractive index: 1.4888 @ 630 nm [14]). The angle of incidence is 80° and the wavelength is 630 nm and s-polarization. The 2D simulations were conducted using COMSOL Multiphysics. b) In-situ AFM image of the pattern transfer of the 5° deflector through t-SPL.

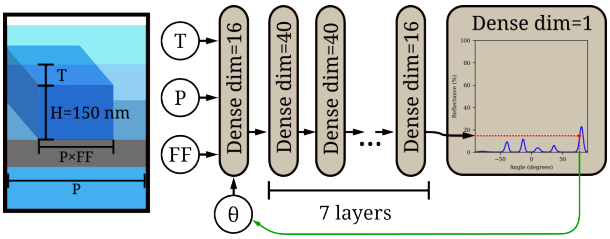

Fig. 2. Schematic of the surrogate model. The activation functions used are sine [15] except the last layer which uses sigmoid. The total training time for the surrogate model was 21 seconds finishing at epoch 167 due to loss not improving by 10^{-6} over 20 epochs. The optimizer of choice for this project was AdamW with initial learning rate 5×10^{-3} [16] and linear scheduler that reduces the learning to 2.5×10^{-7} at epoch 150. The batch size of 360×8.

which took 6 minutes finishing at epoch 494 due to loss not improving by 10^{-8} for 40 epochs. The batch size chosen was 32. The Initial learning rate was 5×10^{-3} and multiplied by 0.99 every epoch.

To obtain the designs we simply prompted the MVANN with artificially generated target responses (80% efficiency). In other words, we crafted the target responses based on the angle we are targeting. Then, we analyse all the solutions for each target with the surrogate model and select the best performing design. After that, a proof of concept using one design optimized for 5° was fabricated, using t-SPL.

III. Fabrication Methodology

Initially, SiO_2-substrates (Corning 2845-18) were cleaned in ultrasonic immersions of acetone and, then, isoprophyl alcohol followed by an O_2 plasma cleaning (Tergeo-EM, PIE Scientific), at 60 sccm. A 300 nm-film of Al was deposited on the substrates via magnetron sputtering (Ulvac MHC-9000, Motorola Solutions Inc).

To fabricate the designed deflectors, t-SPL was used (NanoFrazor Explore, from Heidelberg Instruments). It is a top-down lithography that features sub-20nm high-resolution and maskless patterning [11]. Based on the scanning probe technology, t-SPL relies on the approach of a silicon conical probe (approximate curvature radius of 10 nm) to the surface of a thermally sensitive resist covering the sample by electrostatic actuation. When the probe is in contact with the surface, heat is applied and the resist sublimates according to the desired pattern [17].

We combined the t-SPL methodology with a bilayer liftoff process. Thus, two resists were required: the PMMA/MA (AR-P 617, from Allresist) and phthalaldehyde polymer (PPA) (AR-P 8100, from Allresist). The first one is the liftoff resist whereas the latter, is the thermally sensitive resist which forms the top layer. Both resists were spin coated at 6000 rpm, for 30 s. The PMMA/MA was baked at 180 °C, for 20 min and the PPA, at 110 °C, for 2 min. The thickness of the PPA layer is, approximately, 30 nm whilst the PMMA/MA is 200 nm-thick. It is worth noting that the PMMA/MA layer should be, at least 140% the thickness of the final patterns.

Here, the beam deflector optimized for 5° reflection was fabricated with the aforementioned method. Its fabrication prove the feasibility of implementing the optimization methodology.

The temperature of the scanning probe was set at 880 °C during lithography and the exposure time for each imprinted pixel was 35 µs. Patterning, in the PPA layer, was monitored in real time, with an integrated topography sensor for AFM imaging (Fig. 1b). Then, the sample underwent a downstream O_2 plasma etching and a wet etch in ethyl alcohol to completely expose the underlying Al layer.

In sequence, a film of 150 nm of titania was deposited by magnetron sputtering. Later, an acetone liftoff removed the remaining PMMA/MA. The final sample was, then, rinsed with isoprophyl alcohol (Fig. 3b). The width of each fabricated slab was measured in, approximately, 235 nm with a period of 895 nm. Hence, the dimensions agree with the model at a 10% error.

IV. Results

Fig. 3 a) Shows the optimization results for the fabricated device.

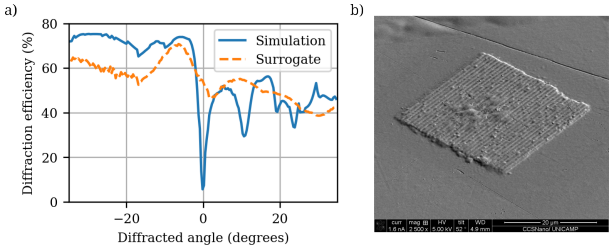

Fig. 3. a) Optimization results for 200 different angles. In the x-axis is plotted the target diffracted angle and on the y-axis the efficiency of the diffracted -1 order mode. The blue curve shows the simulation results with COMSOL Multiphysics and the dashed orange curve represents the surrogate model. Total simulation time: 5 minutes and 10 seconds. b) FIB microscopy of the fabricated device. The bump seen the the center of the device is PMMA/MA that was not fully removed during lift-off.

We analysed two different deflectors in Fig. 4. To see that our algorithm is able to find the global optima on each case despite having multiple local optima. However, in one scenario, despite finding the global maxima, the surrogate model wrongly predicted probably due to a lack of data in the Rayleigh-Wood anomaly [18].

The fabricated device was for the 5°. Having 708 nm of P, indicating 5.5° of deflected angle to the -1 order mode. The filling fraction was 30% and $T = 180$ nm. The simulated efficiency was 52%.

The best use-case for this optimization is for large number of optimizations. Comparing beam deflectors in the literature designed with adjoint optimizations, each optimization would require approximately 80 simulations [10]. Implying that the optimization of 200 devices would require 16 000 simulations instead. For our scenario of small number of parameters, heuristic optimization methods could be more appealing, requiring less iterations while finding the global optima, requiring 30 simulations per optimization in average [19].Once the training simulations are finished and models are trained, the inverse design phase is instantaneous. The biggest disadvantage of

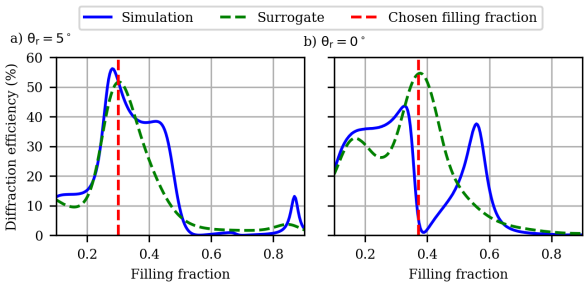

Fig. 4. Analysis on two different cases for optimization. Where we fixed P and T and varied the filling fraction and analysed the results of the simulation and surrogate model. We picked the scenarios of a) $\theta_r = 5°$ and b) $\theta_r = 0°$, which the Rayleigh-Wood anomaly is present [18]. On both cases we observe that our algorithm was able to find the global maxima according to the surrogate model. However, due to lack of data, it showed poor performance, specially for $\theta_r = 0°$. Nevertheless, the methodology was able to capture the global maxima in the dataset, while the surrogate reports slightly modified diffraction efficiencies.

this method is the difference between target and obtained angles. This could be solved by implementing hard constraints on the MVANN.Another disadvantage is the lack of precision of the surrogate model, yielding incorrect responses on points of the dataset with high variations. This measure can be addressed by performing some intelligent sampling. Such as a feedback loop where we add the validation simulations to the dataset and retrain the models. Such alterations will be implemented in future versions of the algorithm.

V. Conclusion

After generating the dataset and training the neural network models, the inverse design becomes simply prompting the model the desired output response. Consequently, with a fixed number of simulations we are able to generate an infinite continuum of designs. In this study, we showcased one design out of 200, each targeting a different angle. The beam deflector at the $5°$-target was fabricated using t-SPL with sub-20 nm resolution. As t-SPL is a direct technique, we can now broaden the study to fabricate several metasurface-based beam deflectors, and proceed with characterization.

References

[1] J. Hu, S. Bandyopadhyay, Y.-h. Liu, and L.-y. Shao, "A review on metasurface: from principle to smart metadevices," *Frontiers in Physics*, vol. 8, p. 586087, 2021.

[2] A. Clini de Souza, S. Lanteri, H. E. Hernandez-Figueroa, M. Abbarchi, D. Grosso, B. Kerzabi, and M. Elsawy, "Back-propagation optimization and multi-valued artificial neural networks for highly vivid structural color filter metasurfaces," *Scientific Reports*, vol. 13, no. 1, p. 21352, 2023.

[3] E. Khaidarov, D. Eschimese, K. H. Lai, A. Huang, Y. H. Fu, Q. Lin, R. Paniagua-Dominguez, and A. I. Kuznetsov, "Large-scale vivid metasurface color printing using advanced 12-in. immersion photolithography," *Scientific Reports*, vol. 12, no. 1, p. 14044, 2022.

[4] Y. Ha, Y. Luo, M. Pu, F. Zhang, Q. He, J. Jin, M. Xu, Y. Guo, X. Li, X. Li *et al.*, "Physics-data-driven intelligent optimization for large-aperture metalenses," *Opto-Electronic Advances*, vol. 6, no. 11, pp. 230 133–1, 2023.

[5] Z.-B. Fan, Y.-F. Cheng, Z.-M. Chen, X. Liu, W.-L. Lu, S.-H. Li, S.-J. Jiang, Z. Qin, and J.-W. Dong, "Integral imaging near-eye 3d display using a nanoimprint metalens array," *eLight*, vol. 4, no. 1, p. 3, 2024.

[6] J. C. Zhang, Y. Fan, J. Yao, M. K. Chen, S. Lin, Y. Liang, B. Leng, and D. P. Tsai, "Programmable optical meta-holograms," *Nanophotonics*, vol. 13, no. 8, pp. 1201–1217, 2024.

[7] M. M. Elsawy, S. Lanteri, R. Duvigneau, J. A. Fan, and P. Genevet, "Numerical optimization methods for metasurfaces," *Laser & Photonics Reviews*, vol. 14, no. 10, p. 1900445, 2020.

[8] P. R. Wiecha, A. Arbouet, C. Girard, and O. L. Muskens, "Deep learning in nano-photonics: inverse design and beyond," *Photonics Research*, vol. 9, no. 5, pp. B182–B200, 2021.

[9] A. C. de Souza, S. Lanteri, H. E. Hernandez-Figueroa, M. Abbarchi, D. Grosso, B. Kerzabi, and M. Elsawy, "Inverse design of bright, dielectric metasurfaces color filters based on back-propagation and multi-valued artificial neural networks," in *Machine Learning in Photonics*, vol. 13017. SPIE, 2024, pp. 62–71.

[10] P. Dainese, L. Marra, D. Cassara, A. Portes, J. Oh, J. Yang, A. Palmieri, J. Rodrigues, A. Dorrah, and F. Capasso, "Shape optimization for high efficiency metasurfaces: theory and implementation," *arXiv preprint arXiv:2405.03930*, 2024.

[11] S. T. Howell, A. Grushina, F. Holzner, and J. Brugger, "Thermal scanning probe lithography—a review," *Microsystems & nanoengineering*, vol. 6, no. 1, p. 21, 2020.

[12] J. H. Halton, "On the efficiency of certain quasi-random sequences of points in evaluating multi-dimensional integrals," *Numerische Mathematik*, vol. 2, pp. 84–90, 1960.

[13] A. B. Owen, "A randomized halton algorithm in r," *arXiv preprint arXiv:1706.02808*, 2017.

[14] N. Sultanova, S. Kasarova, and I. Nikolov, "Dispersion properties of optical polymers," *Acta Physica Polonica A*, vol. 116, no. 4, pp. 585–587, 2009.

[15] V. Sitzmann, J. Martel, A. Bergman, D. Lindell, and G. Wetzstein, "Implicit neural representations with periodic activation functions," *Advances in neural information processing systems*, vol. 33, pp. 7462–7473, 2020.

[16] I. Loshchilov and F. Hutter, "Decoupled weight decay regularization," *arXiv preprint arXiv:1711.05101*, 2017.

[17] E. Albisetti, A. Calò, A. Zanut, X. Zheng, G. M. de Peppo, and E. Riedo, "Thermal scanning probe lithography," *Nature Reviews Methods Primers*, vol. 2, no. 1, p. 32, 2022.

[18] R. W. Wood, "Xlii. on a remarkable case of uneven distribution of light in a diffraction grating spectrum," *The London, Edinburgh, and Dublin Philosophical Magazine and Journal of Science*, vol. 4, no. 21, pp. 396–402, 1902.

[19] M. M. Elsawy, M. Binois, R. Duvigneau, S. Lanteri, and P. Genevet, "Optimization of metasurfaces under geometrical uncertainty using statistical learning," *Optics Express*, vol. 29, no. 19, pp. 29 887–29 898, 2021.